Waveform Codesign for Radar−Communication Spectral Coexistence via Dynamic Programming

Article *in* IEEE Transactions on Aerospace and Electronic Systems · October 2022

DOI: 10.1109/TAES.2022.3162567

Shammi A. Doly
Arizona State University

Alex Chiriyath
Arizona State University

Hans Mittelmann
Arizona State University

Dan Bliss
Arizona State University

This article has been accepted for publication in a future issue of this journal, but has not been fully edited. Content may change prior to final publication. Citation information: DOI 10.1109/TAES.2022.3162567, IEEE Transactions on Aerospace and Electronic Systems

Waveform codesign for radar-communications spectral coexistence via dynamic programming

Shammi A. Doly *, Alex Chiriyath*, Hans D. Mittelmann†, Daniel W. Bliss* and Shankarachary Ragi‡
* School of Electrical, Computer and Energy Engineering, Arizona State University, Tempe, AZ 85287
Email: sdoly@asu.edu, achiriya@asu.edu & d.w.bliss@asu.edu
† School of Mathematical and Statistical Sciences, Arizona State University, Tempe, AZ 85287
Email: mittelmann@asu.edu
‡ Department of Electrical Engineering, South Dakota School Mines & Technology, Rapid City, SD 57701
Email: shankarachary.ragi@sdsmt.edu

***Abstract*—We develop a new waveform codesign approach for radar-communications spectral coexistence using a decision-theoretic framework called *partially observable Markov decision process* (POMDP). The POMDP framework's natural look-ahead feature allows us to trade-off short-term for long-term performance, which is necessary in waveform codesign problems with competing objectives and dynamic user needs. As POMDPs are computationally intractable, we extend two approximation methods called *nominal belief-state optimization* and *random-sampling multipath hypothesis propagation* to make the codesign approaches tractable.**

I. Introduction

Spectral congestion is forcing legacy radar band users to investigate cooperation and co-design methods with a growing number of communications applications [1]. The codesign of radar and wireless communications systems faces several challenges: interference, radar, communications decoupling, and dynamic user (radar and communications) requirements. The studies in [2], [3] provide a detailed overview of the challenges and research directions in the "spectral" coexistence of radar and communications. In the study in [4], the quality of the radar return and the communications rate is mainly determined by the waveform's spectral shape. Moreover, one of the critical challenges for any waveform design method is to meet dynamic user needs. In this paper, we develop waveform shaping methods that are adaptive and can trade-off between competing performance objectives to address these challenges. A waveform design method can most effectively meet the dynamic user needs if it predicts the future user needs and allocates the resources accordingly. Previous research has considered waveform design for joint radar-communications systems, for example, [5], [6]. However, existing methods often do not meet dynamic performance requirements, as they tend to be *greedy* in that they only maximize short-term performance for immediate benefits. For problems with dynamic performance requirements, long-term performance is critical as decisions (to choose a particular waveform) at the current time epoch may lead to regret in the future. To address these challenges, we develop an adaptive waveform design method for joint radar-communications systems based on the theory of *partially observable Markov decision process* (POMDP) [7], [8]. Specifically, we formulate the waveform design problem as a POMDP [8], after which the design problem becomes a matter of solving an optimization problem. In essence, the POMDP solution provides us with the optimal decisions on the waveform design parameters [9]. The optimization problems resulting from POMDPs are hard to solve precisely; specifically, these problems are PSPACE-complete [10]. The optimization problems resulting from POMDP formulation are typically reformulated as *dynamic programming* problems, which allows us to apply *Bellman's principle of optimality*, leading to a plethora of approximation methods called *approximate dynamic programming* methods or ADP methods as surveyed in [7]. In this study, we adopt two different ADP approaches called nominal belief-state optimization (NBO) [7], and *random sampling multipath hypothesis propagation* (RS-MHP) [11], [12] to maximize the reward in the long horizon decision problems. RS-MHP methods are a variant of the existing broad class of Monte-Carlo tree search (MCTS) methods. The POMDP framework has a natural look-ahead feature, i.e., it can trade-off short-term for long-term performance. This feature lets the POMDP naturally anticipate the dynamic user needs and optimize the resources (waveforms) to actively meet the user's needs. Typically, one studies these adaptive methods under "cognitive radio (radar)," which has a rich literature. The current waveform design problem is related to a class of problems called *adaptive sensing*, where POMDP was already a proven effective framework [9], [13]. However, this paper brings formalism to these methods by posing the waveform design problem as a POMDP. Recently, POMDPs were used in [14] to develop adaptive methods for "cognitive radar," but in a different context, where the focus was on optimizing radar measurement times and not on waveform

The work of S. Doly, S. Ragi, and H. D. Mittelmann was supported in part by the Air Force Office of Scientific Research under grant FA9550-19-1-0070.

shaping.

A. Literature Review

Modern spectrum sharing techniques proposed waveform co-design and operation as a necessary construct for joint radar-communications [15], [16]. Various methods employ optimization theory to select a jointly optimal waveform [17]–[19] or jointly maximizing information criteria for radar and orthogonal frequency-division multiplexing (OFDM) communications users to minimize mutual interference for dynamic bandwidth allocation [20]. Other avenues for co-design have also been investigated [21]–[30]. Most modern co-design approaches do not take the long term needs of the system into consideration. The proposed POMDP-based waveform co-design framework is able to evaluate the needs of the system into the future and trade performance in the short-term versus the long-term.

Cognitive techniques in radar were primarily used for enhanced dynamic behavior in complex environments [31], [32], but researchers have begun to look at cognitive radar as a solution to the spectral scarcity problem via radar scheduling [33] or employing cognitive radio spectrum sensing techniques, emitter localization, and power allocation to avoid interference [34]–[39]. Others have investigated cognitive radar as a solution to the spectral congestion problem [40]–[43]. Most research efforts tend to adaptively use the spectrum to avoid interference. Such methods are akin to the traditional spectrum sharing solution of isolation in space, time and/or frequency, which can limit joint system performance as opposed to a co-design approach, where both systems cooperatively utilize the spectrum. Co-design approaches, such as our POMDP-based approach, show better joint system performance due to better cooperation between systems.

Relationships between radar estimation sidelobe ambiguity and communications channel coding were previously studied [44]. Others have suggested specific coding techniques with favorable properties such as finite Heisenberg-Weyl groups [45], Golay waveforms with Doppler resilient properties [46], and complementary sequences [47]. These approaches tend to prioritize the performance of one system over the other, and as such are sub-optimal in performance to most modern co-design approaches.

OFDM was investigated as a viable option in vehicle-to-vehicle applications [48]–[51], software-defined radio (SDR) architectures [52], etc. However, results show conflicting cyclic prefix requirements, data-dependent ambiguities, and trouble mitigating peak-to-average power ratio (PAPR) for typical radar power requirements. Researchers focused on developing joint systems that could mitigate the effects of these problems, such as suppressing side-lobes [53], maintaining a constant envelope [54], or reducing PAPR [55]. An OFDM approach is fundamentally more favorable to communications system performance and most research efforts lie in improving radar performance to an acceptable level. However, co-design approaches such as ours are more beneficial in the long-term due to them giving both systems equal importance.

TABLE I: Survey of Notation

Variable	Description
B	Total system bandwidth
B_{rms}	Root-mean-squared radar bandwidth
B_{com}	Communications-only subband
P_{rad}	Radar power
T_{temp}	Effective temperature
b	Communications propagation loss
P_{com}	Communications power
P_{rad}	Communications power
$x(t)$	Unit-variance transmitted radar signal
a	Combined antenna gain
N	Number of samples
σ^2_{CRLB}	Cramer-Rao lower bound
σ^2_{noise}	Thermal noise
σ^2_{proc}	Process noise variance
TB	Time-bandwidth product
δ	Radar duty factor
w	Measurement noise
ζ_k	Mean vector noise
τ	Time delay to m^{th} target
α	Weighting parameter
R_{comm}	Communications rate
R_{est}	Radar estimation rate
P_k	Error covariance matrix
T_{pri}	Pulse repetition interval
H	Planning horizon length

B. Key Contributions

Below are the key contributions of this study.

- We formulate the joint radar waveform codesign problem as a POMDP.
- We extend ADP methods NBO and RS-MHP to solve the waveform design problem posed as POMDP.
- We implement the POMDP-based waveform codesign algorithms in simulated environments and conduct a numerical study to quantify the impact of the planning horizon on the performance of our methods.

A preliminary version of the parts of this paper was published as [8]. This paper differs from the conference paper [8] in the following ways: 1) along with the previous numerical results in [8] we conduct an empirical study to assess the impact of the planning horizon H in POMDP on the radar and communications performance; 2) we extend a new ADP approach RS-MHP [11], [12] to solve the waveform codesign problem, and benchmark its performance against the NBO approach we previously used in [8].

This article has been accepted for publication in a future issue of this journal, but has not been fully edited. Content may change prior to final publication. Citation information: DOI 10.1109/TAES.2022.3162567, IEEE Transactions on Aerospace and Electronic Systems

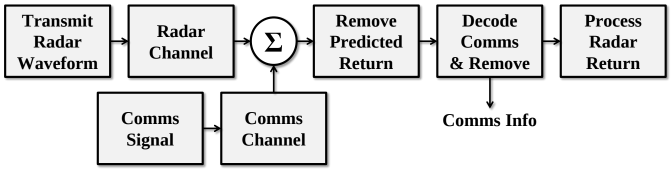

Fig. 1: Joint radar-communications system block diagram for SIC scenario. The radar and communications signals have two effective channels, but arrive converged at the joint receiver. The radar signal is predicted and removed, allowing a reduced rate communications user to operate. Assuming near perfect decoding of the communications user, the ideal signal can be reconstructed and subtracted from the original waveform, allowing for unimpeded radar access.

II. Joint-Radar Communications Premise

A. Successive Interference Cancellation Receiver Model

Table I shows the notations employed in this paper. In this study, we use an optimal multi-user receiver model called successive interference cancellation (SIC) [2], [57] to remove the communication signal from the radar return. Based on the prior observations of the radar target range (or time-delay) up to some random fluctuation (also called process noise) $n_{\mathrm{proc}}(t)$ as a zero-mean random variable we generate the radar return. Then we subtract the predicted radar return from the joint radar-communications signal received. After suppressing the radar return, the receiver then decodes and removes the communications signal from the received signals. It is this receiver model that causes communications performance to be closely tied to the radar waveform spectral shape. The block diagram of the joint radar-communications system considered in this scenario is shown in Figure 1. When applying SIC, the interference residual plus noise signal $n_{\mathrm{int+n}}(t)$, from the communications receiver's perspective, is given by [3], [58]

$$\begin{aligned} n_{\mathrm{int+n}}(t) &= n(t) + n_{\mathrm{resi}}(t) \\ &= n(t) + \sqrt{\|a\|^2 \, P_{\mathrm{rad}}} \, n_{\mathrm{proc}}(t) \, \frac{\partial x(t-\tau)}{\partial t}, \end{aligned} \quad (1)$$

and

$$\|n_{\mathrm{int+n}}(t)\|^2 = \sigma^2_{\mathrm{noise}} + a^2 \, P_{\mathrm{rad}} \, (2\pi \, B_{\mathrm{rms}})^2 \, \sigma^2_{\mathrm{proc}} \,, \quad (2)$$

where $n_{\mathrm{proc}}(t)$ is the process noise with variance σ^2_{proc}.

B. Radar Estimation Rate

To measure spectral efficiency for radar performance, we developed a new metric recently called *radar estimation rate*, which is formally defined as the minimum average data rate required to provide time-dependent estimates of system or target parameters, for example, target range [3], [58], [59]. The radar estimation rate is expressed as follows:

$$R_{\mathrm{est}} = I(\mathbf{x};\mathbf{y})/T_{\mathrm{pri}}, \quad (3)$$

where $I(\mathbf{x};\mathbf{y})$ is the mutual information between random vectors $\mathbf{x}$ and $\mathbf{y}$, and T_{pri} $=T_{\mathrm{pulse}}/\delta$ is the pulse repetition interval of the radar system, T_{pulse} is the radar pulse duration, and δ is the radar duty factor. This rate allows construction of joint radar-communications performance bounds, and allows future system designers to score and optimize systems relative to a joint information metric. For a simple range estimation problem with a Gaussian tracking prior, this takes the form [2], [3], [60]:

$$R_{\mathrm{est}} = (1/2T)\log_2(1 + \sigma^2_{\mathrm{proc}}/\sigma^2_{\mathrm{CRLB}}), \quad (4)$$

where σ^2_{proc} is the range-state process noise variance and σ^2_{CRLB} is the Cramér-Rao lower bound (CRLB) for range estimation given by [3], [58], [59]

$$\sigma^2_{\mathrm{CRLB}} = \frac{\sigma^2_{\mathrm{noise}}}{8\pi^2 \, B^2_{\mathrm{rms}} \, T_p \, B \, P_{\mathrm{rad,rx}}} \quad (5)$$

where $\sigma^2_{\mathrm{noise}}$ is the noise variance or power, T_p is the radar pulse duration, B_{rms} is the radar waveform root mean square (RMS) bandwidth, and $P_{\mathrm{rad,rx}}$ is the radar receive power, which is inversely proportional to the distance of the target from the joint node. Immediately apparent is the similarity of above equation to Shannon's channel capacity equation [3], [58], [59], where the ratio of the source uncertainty variance to the range estimation noise variance forms a pseudo-signal-to-noise ratio (SNR) term. In Eq. 4, the estimation rate is inversely proportional to the distance of the target from the joint node. As discussed later, we design the waveform parameters over the planning horizon while accounting for the varying estimation rate due to target's motion.

C. Inner rate bounds

We measure the performance of the system with two metrics: communications information rate bound and radar estimation rate bound (discussed in the previous section). The joint radar-communications performance bounds developed in [3], [58], [59] considered only local radar estimation error, therefore making simplified assumptions about the radar waveform. In [4], the results were generalized to include formulation of an optimal radar waveform for both global radar estimation rate performance and consideration of in-band communications users forced to mitigate radar returns. After the SIC process, some radar residual will be left in the communications signal (due to error in predicted target location and actual target location). If $R_{est} \approx 0$ is sufficiently low, then the communications operates according to the bound determined by the isolated communications system [2]. The highest possible communications rate when decoding the post-SIC received signal is given by

$$\tilde{R}_{\mathrm{com}} \leq B \log_2 \left[1 + \frac{b^2 P_{\mathrm{com}}}{\sigma^2_{\mathrm{noise}}}\right]. \quad (6)$$

If $\tilde{R}_{com}$ is sufficiently low for a given transmit power then the communications signal can be decoded and subtracted

This article has been accepted for publication in a future issue of this journal, but has not been fully edited. Content may change prior to final publication. Citation information: DOI 10.1109/TAES.2022.3162567, IEEE Transactions on Aerospace and Electronic Systems

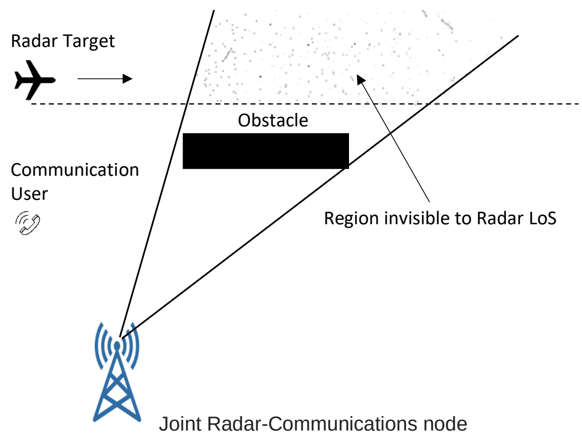

Fig. 2: Target tracking problem scenario

completely from the underlying signal, so that the radar parameters can be estimated without contamination,

$$\tilde{R}_{\text{com}} \leq B \log_2 \left[1 + \frac{b^2 P_{\text{com}}}{\sigma^2_{\text{noise}} + a^2 \, P_{\text{rad}} \, (2\pi \, B_{\text{rms}})^2 \, \sigma^2_{\text{proc}}} \right], \tag{7}$$

In this regime, the corresponding estimation rate bound R_{est} is given by Eq. 4. An achievable rate lies within the imaginary triangle constructed by the Eq. 4, Eq. 6, and Eq. 7.

III. Problem Specification

We consider a case study with a radar target, communications user, and the joint node, as shown in Figure 2. We consider a single clutter condition as shown in Figure 2 where an obstacle may occlude the line-of-sight of the target from the joint node. Total clutter residue acts as extra additive noise in the system, which causes the channel to appear more degraded. Radar estimation rates are also reduced (radar and communications overlap) once the clutter occludes the target. We do not consider any external interference or a jamming condition in this paper. We will develop our POMDP framework for this case study, which can be easily generalized and extended to other problem scenarios. This particular case study allows us to show the qualitative and quantitative benefits of POMDP in adaptive waveform design. The key components in the waveform design algorithm based on POMDP are shown in Figure 3. The POMDP planner evaluates the belief-state (posterior distribution over the state space updated according to Bayes' rule) of the system, uses an ADP method to solve the POMDP approximately, and produces optimal or near-optimal decisions on waveform parameters; details are discussed later. Our objective is to design the shape of the waveforms over time to maximize the system's performance. First, we begin with a unimodular chirp waveform $\exp[j(\pi B/T)(t^2)]$. We control the spectral shape of this chirp signal to maximize joint performance. We first sample the chirp signal and collect m samples in the frequency domain to achieve this. Let $X = (X(f_1), \ldots, X(f_m))^T$ be the discretized signal in the frequency domain at frequencies $f_1, \ldots, f_m$. Let $u = (u(1), \ldots, u(m))^T$ be an array of spectral weights we will optimize as discussed below, where $u(i) \in [0, 1], \forall i$. We control the chirp signal's spectral shape by multiplying (i.e., dot product) the signal with the spectral weights in the frequency domain, i.e., the resulting signal is given by $X(f_i)u(i), \forall i$.

IV. POMDP Formulation for Joint Waveform Codesign

To pose any decision making problem as a POMDP, we need to define the POMDP ingredients, namely states, actions, state-transition law, observations and observation law, and reward function, in the context of the particular problem at hand. Below is a description of the POMDP ingredients as defined specific to our waveform design problem. Hereafter, we model the system dynamics as a discrete event process, where k represents the discrete time index.

States: State at time k is defined as $x_k = (\chi_k, \xi_k, P_k)$, where χ_k represents the target state, which includes the location, velocity, and the acceleration of the target; and (ξ_k, P_k) represents the state of the tracking algorithm, e.g., Kalman filter, where ξ_k is the mean vector, and P_k is the covariance matrix.

Actions: Actions are the waveform spectral weights vector u_k, at time k, as defined previously.

State-Transition Law: χ_k evolves according to a target motion model *near-constant velocity model* [9] captured by $\chi_{k+1} = F\chi_k + n_k$, where F is a transition matrix, and $n_k = n_{\text{proc}}(t = k)$ is the process noise described in Section II-A, which is modeled as a Gaussian process. ξ_k and P_k evolve according to Kalman filter equations. **Observation Law**: $z_k^{\text{Targ}} = G\chi_k + w_k$ (if not occluded) and $z_k^{\text{Targ}} = w_k$ (if occluded), where G is a transition matrix, and w_k is the measurement noise, modeled as a Gaussian process. Specifically, $w_k \sim \mathcal{N}(0, R_k)$, where R_k is the noise covariance matrix, where the entries in the matrix scale (increase) with the distance between the joint node (or sensor node) and the target. We assume the other state variables to be fully known.

Reward Function: The reward function rewards the decision u_k taken at time k given the state of the system is x_k as defined below:

$$R(x_k, u_k) = \alpha R_{\text{est}}(x_k, u_k) + (1-\alpha) R_{\text{comm}}(x_k, u_k) \tag{8}$$

where R_{est} is the radar estimation rate [4], R_{comm} is the communications data rate, and $\alpha \in [0, 1]$ is a weighting parameter. The dependence of the rates on the waveform spectral weights u_k is explained as follows. Both the rates $R_{\text{est}}(x_k, u_k)$ and $R_{\text{comm}}(x_k, u_k)$ is a function of the RMS bandwidth B_{rms} of the waveform as can be seen from equations 4, 5, and 7. The RMS bandwidth clearly depends on the shape of the waveform spectrum, which is determined by the waveform spectral weights u_k.

This article has been accepted for publication in a future issue of this journal, but has not been fully edited. Content may change prior to final publication. Citation information: DOI 10.1109/TAES.2022.3162567, IEEE Transactions on Aerospace and Electronic Systems

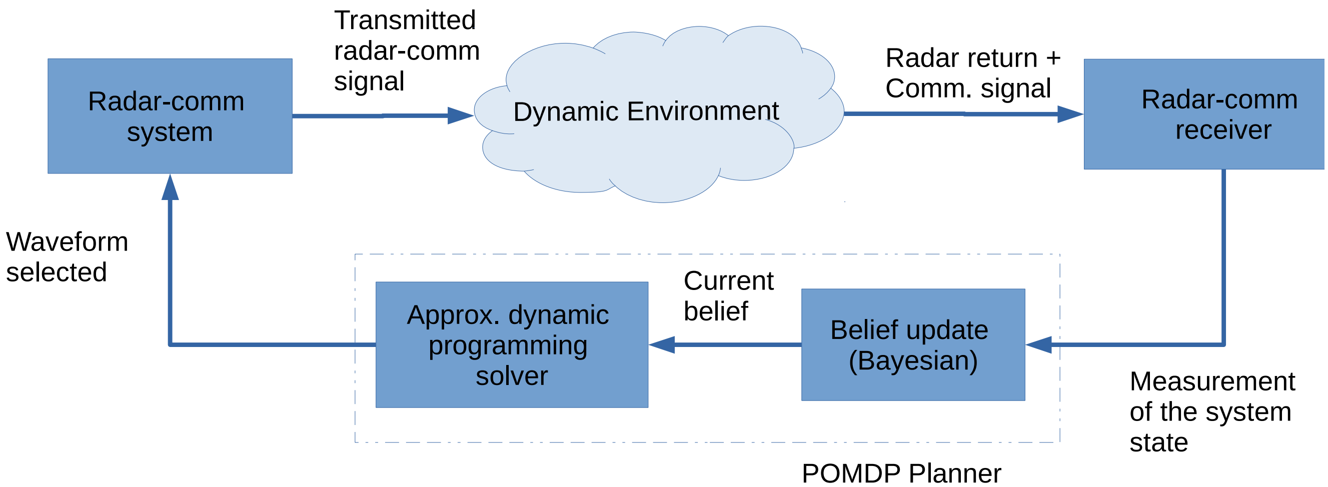

Fig. 3: Adaptive waveform optimization in a dynamic environment.

Belief State: We maintain and update the posterior distribution over the state space (as the actual state is not fully observable), also known as the "belief state" given by $b_k = (b_k^\chi, b_k^\xi, b_k^P)$, where $b_k^\xi(x) = \delta(x - \xi_k)$, $b_k^P(x) = \delta(x - P_k)$, and $b_k^\chi = \mathcal{N}(\xi_k, P_k)$. Here, we know the state of the tracking algorithm, so belief states corresponding to these states are just delta functions, whereas the target state is modeled as a Gaussian distribution with ξ_k and P_k as the mean vector and the error covariance matrix respectively. Our goal is to optimize the actions over a long time-horizon (of length H) to maximize the expected cumulative reward. The objective function (to be maximized) is given by $J_H = \mathrm{E}\left[\sum_{k=0}^{H-1} R(x_k, u_k)\right]$. But, we can also write J_H in terms of the belief states as

$$J_H = \mathrm{E}\left[\sum_{k=0}^{H-1} r(b_k, u_k) \,\middle|\, b_0\right], \tag{9}$$

where, $r(b_k, u_k) = \int R(x, u_k) b_k(x)\,\mathrm{d}x$ and b_0 is the initial belief state. Let $J_H^*(b)$ represent the optimal objective function value, given the initial belief-state b. Therefore, the optimal action policy at time k is given by $\pi^*(b_k) = \arg\max_u Q(b_k, u)$, where $Q(b_k, u) = r(b_k, u) + \mathrm{E}\left[J_H^*(b_{k+1}) \,|\, b_k, u\right]$ which is also called the Q-value. A detailed description of POMDP and its solution can be found in [7], [9]. POMDP formulations are notorious for their high computational complexity (PSPACE-complete [10]), particularly because it is near impossible to obtain the above-discussed Q-value in real-time [9]. Most ADP methods approximate the Q-value [7]. We adopt two ADP approaches: *nominal belief-state optimization* (NBO) [9] and *random sampling - multipath hypothesis propagation* (RS-MHP) [11], [12].

Algorithm 1 Nominal Belief State Optimization (NBO) Algorithm

Require: Find the (sub)optimal spectral weights using the NBO approach at a discrete-time index k

Initialize the environment, noise intensities, process noise matrix
$H \leftarrow$ length of planning horizon
$k \leftarrow$ discrete-time index
Initialize action vector u_k to random spectral weights, and the prior belief state is b_k
Define the NBO objective/reward function: $J_{NBO}(u_k) \leftarrow$ cumulative (over planning horizon H) weighted average of the estimation and communications rates (see Eq. 10), where the estimation and communications rates are evaluated assuming the future target belief states are evaluated with all noise variables collapsing to their "nominal values"
for each k **do**
  Update the target belief state b_k (posterior distribution) via Kalman-Bayes equations using the target state measurements received at k
  Solve the below NBO optimization problem to obtain the (sub)optimal weights using MATLAB's *fmincon*: $u_k^* \leftarrow \arg\max_u J_{NBO}(u)$
  Design the spectral shape of the chirp signal using optimal weights u_k^* as discussed in Section III
end for ▷ k

A. POMDP Solution via NBO

With NBO approximation, the POMDP formulation leads to the following optimization problem:

$$\max_{u_k, k=0,\ldots,H-1} \sum_{k=0}^{H-1} r(\tilde{b}_k, u_k), \tag{10}$$

This article has been accepted for publication in a future issue of this journal, but has not been fully edited. Content may change prior to final publication. Citation information: DOI 10.1109/TAES.2022.3162567, IEEE Transactions on Aerospace and Electronic Systems

where $\tilde{b}_k, k = 0, \ldots, H-1$ is a sequence of readily available "nominal" belief states, as opposed to b_ks which are random variables, obtained from the NBO approach. In NBO, the expectation is replaced by a sample state trajectory generated with an assumption that the future noise variables in the system collapse to the nominal or mean values (Figure 4), thus making the above objective function deterministic. The NBO method was developed to solve a UAV path optimization problem, which was posed as a partially observable Markov decision process (POMDP) [9]. POMDP generalizes the long horizon optimal control problem described in [11] in that the system state is assumed to be "partially" observable, which is inferred via the use of noisy observations and Bayes rules. Although the performance of the NBO approach was satisfactory in that it allowed to obtain reasonably optimal reward commands for the decision problem to be received, it ignored the uncertainty due to noise disturbances, thus leading to inaccurate evaluation of the objective function. This challenge can be overcome by the RS-MHP approach as discussed below.

B. POMDP solution via RS-MHP

The tree-like sampling of the states in the RS-MHP approach, as shown in figures 4 and 5, allows us to incorporate the uncertainty of the state evolution into the decision-making criteria, albeit with the increased computational burden compared to NBO. However, the sampling approach allows us to trade-off between the computational intensity and the solution's optimality (determined by our choice of the number of samples/branches in RS-MHP). In RS-MHP approach, we sample the probability distribution of the state of the system (a random variable) N times at each time step and generate a sampling tree as shown in Figure 5 (here, $N = 3$). To avoid the exponential growth of the state sample nodes in this approach, at each time step we retain only M sample states and prune the remaining samples. If the number of the sample states at a given time instance is less than or equal to M, we do not perform pruning. Figure 5 shows an illustration of the above branch pruning strategy for a scenario with $N = 3$ and $M = 3$. We prune the tree branches based on their likeliness indices [11], [12], i.e., we retain the top M branches at each time step with the highest sample probabilities. We approximate the expectation with an average over the possible state trajectories or tree branches as follows:

$$J_{RS-MHP} = \frac{1}{M}\sum_{i=1}^{M}\left(\mathrm{E}\left[\sum_{k=0}^{H-1} r(x_k^i, u_k)\,\middle|\, b_0\right]\right) \qquad (11)$$

where x_k^i represents the sample state node from the ith trajectory at time k. Clearly, as $N \to \infty$ and $M \to \infty$, the above approximation converges to the true objective function in Eq. (9).

Algorithm 2 Random Sampling Multipath Hypothesis Propagation (RS-MHP) Algorithm

Require: Find the (sub)optimal spectral weights using the RS-MHP approach at a discrete-time index k

Initialize the environment, noise intensities, process and measurement matrix
$H \leftarrow$ length of planning horizon
$k \leftarrow$ discrete-time index
$N \leftarrow$ sampling size (as described in Section IV-B)
$M \leftarrow$ retained states after pruning (as described in Eq. 11)
Initialize action vector u_k to random spectral weights, and the prior belief state be b_k
Define the RS-MHP objective/reward function: $J_{RS-MHP}(u_k) \leftarrow$ cumulative (over planning horizon H) reward function averaged over all the possible state trajectories or tree branches (see Eq. 11), where the estimation and communications rates are evaluated assuming the future target belief states are evaluated using the sampling procedure discussed in Section IV-B.
for each k **do**
    update the target belief state b_k (posterior distribution) via Kalman-Bayes equations using the target state measurements received at time k
    Solve the below optimization problem to obtain the (sub)optimal weights using MATLAB's *fmincon*: $u_k^* \leftarrow \arg\max_u J_{RS-MHP}(u)$
    Design the spectral shape of the chirp signal using optimal weights u_k^* as discussed in Section III.
end for $\triangleright$ k

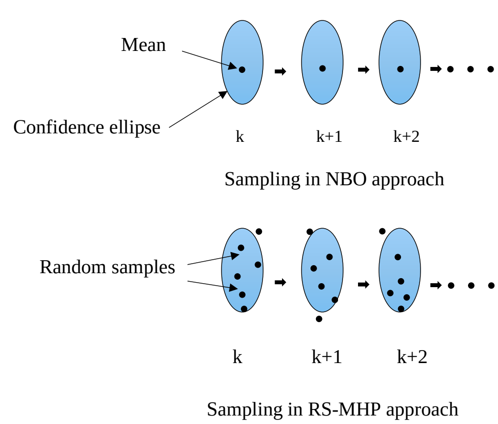

Fig. 4: Sampling in NBO vs. RS-MHP approach

This article has been accepted for publication in a future issue of this journal, but has not been fully edited. Content may change prior to final publication. Citation information: DOI 10.1109/TAES.2022.3162567, IEEE Transactions on Aerospace and Electronic Systems

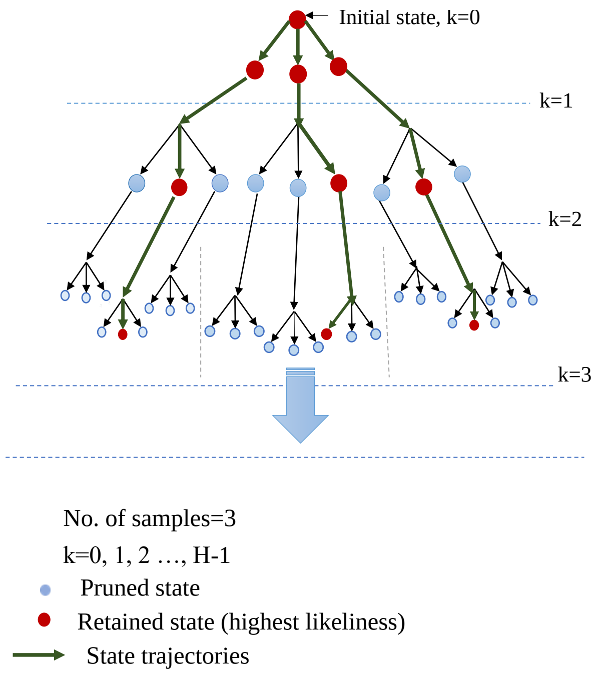

Fig. 5: Sampling in RS-MHP approach with pruning (3 nodes allowed to remain at each stage).

V. Simulation and Results

We study the efficacy of the above-mentioned waveform codesign methods in a scenario with two obstacles blocking the line-of-sight (LOS) between the joint node and the radar target as the target moves from the left to the right, as shown in Figure 7. Furthermore, we implement the receding horizon control approach while optimizing the decision variables over the moving planning horizon [9]. We implement the NBO & RS-MHP approaches to solve the joint radar waveform optimization problem, in the above context, in MATLAB. We use MATLAB's *fmincon* [61] (an optimization tool in MATLAB) to solve the optimization problems discussed in the previous section. The following are the main objectives of this numerical study.

- Study the optimal radar waveform properties.
- Study the impact of the planning horizon H on the joint performance with respect to the estimation and the communications rates.
- Performance comparison of NBO vs. RS-MHP ADP approaches in the non-myopic approach ($H > 1$).

A. Optimal radar waveform properties

We assume that the joint radar-communications receiver shares a single antenna front end and that the communications signal is received through an antenna sidelobe while the radar return is received through the same antenna mainlobe, so that the radar and communications receive gain are not identical. From the simulation results, the SNR in the NBO approach is 19.1419dB, and the RS-MHP approach is 22.4310dB.

TABLE II: Parameters for Waveform Design Methods

Parameter	Value
Bandwidth (B)	5 MHz
Center frequency	3 GHz
Effective temperature (T_{temp})	1000 K
Communications range	10 km
Communications power (P_{com})	1 W
Communications receiver Side-lobe gain	20 dBi
Radar antenna gain	30 dBi
Target cross section	10 m^2
Target process standard deviation (σ_{proc})	100 m
Time-bandwidth product (TB)	128
Radar duty factor (δ)	0.01

The parameters used in our simulation studies are shown in Table II. In Figure 6 (a) we show the radar waveform spectral autocorrelation function of optimized waveform with blending parameter $\alpha = 0.5$ and planning horizon $H = 1$ at a time step $k = 1$. We plot the spectrum of the optimized waveform with $\alpha = 0.5$ along with the original unmasked chirp waveform as shown in Figures 6 (b). This waveform spectrum shows the joint radar-communications optimal and has more energy at the bandwidth center than the sidebands. Radar waveform spectrum with $\alpha = 0.1$ and $\alpha = 1$ along with the original unmasked chirp waveform shown in Figure 8.

B. Effect of planning horizon length on the joint performance

We implement the NBO approach for $H = 1$ and $H = 9$ as shown in Figure 7. In both cases, the size of the error confidence ellipse of the target increases when the target is occluded by the obstacles. The growth of the ellipse size visibly reduces for $H = 9$ compared to $H = 1$. So, the non-myopic method ($H > 1$) has a better capability in keeping the growth of the target-sate uncertainty small compared to a myopic approach ($H = 1$). Figure 9 shows the estimation and the communications rates as a function of the blending parameter α. As expected, α allows us to smoothly trade-off between the two rates. Furthermore, in Figure 10, we plot the estimation rate as a function of time for the above two scenarios with $H = 1$ and $H = 9$, which shows the quantitative benefit of a non-myopic approach ($H > 1$) over a myopic approach ($H = 1$) in terms of the radar estimation rate. Figure 11 shows a gradual increase in the joint radar-communications performance with increasing H as expected in a non-myopic approach, however, the computational complexity in solving Eq. 9 grows exponentially with H.

C. Performance comparison of NBO vs. RS-MHP ADP approaches

Here we implement the RS-MHP approach for waveform codesign in the same simulation scenario described earlier. Figure 12 shows the cumulative distribution of the radar

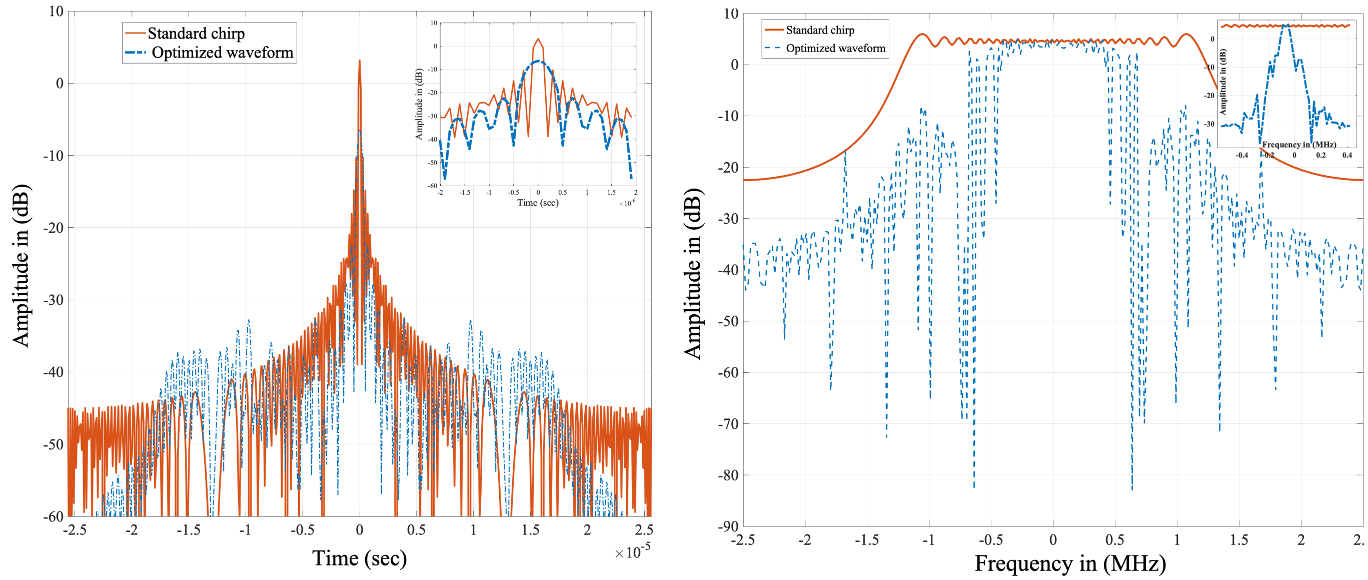

(a) Radar waveform autocorrelation function of the optimized waveform with $\alpha = 0.5$ and $H = 1$

(b) Radar waveform spectrum with $\alpha = 0.5$ and $H = 1$. The standard chirp is depicted by the red line, and the optimal waveform spectrum is shown by the blue dotted line

Fig. 6: Optimized waveform vs. the standard chirp.

estimation rates using RS-MHP and NBO methods for $H = 3$. The figure clearly demonstrates that the RS-MHP approach outperforms the NBO approach and that the performance improves as we increase the number of samples N in the RS-MHP approach. Figure 13 shows the average radar estimation rates for N set to 10, 50, 100, 150, and 200 for $H = 3$. The figure shows a gradual increase in the algorithm's performance (in terms of the estimation rate) with increasing N as expected. This result also suggests that the pruning step in RS-MHP method would degrade the performance but can provide gains in terms of computational intensity. In summary, our numerical study confirms that the RS-MHP's performance has a clear statistical edge over that of the NBO approach in terms of the estimation rate.

VI. CONCLUSIONS

We developed a waveform codesign approach for joint-radar communications systems using a decision-theoretic framework called *partially observable Markov decision processes* (POMDPs). The goal is to optimize the spectral shape of the radar waveform over time to maximize the joint performance of radar and communications in spectral coexistence measured in terms of radar estimation and communications rates. As most decision-theoretic formulations suffer from the *curse of dimensionality*, we extended two approximation strategies or *approximate dynamic programming* (ADP) methods to solve the POMDP - *nominal belief-state optimization* (NBO) and *random sampling multipath hypothesis propagation* (RS-MHP). Our numerical study confirmed that the POMDP-based non-myopic waveform codesign approach has a better capability in keeping the growth of target state uncertainty small compared to a myopic approach. We also presented the quantitative benefits, in terms of the communications and the radar estimation rates, of our POMDP-based non-myopic approach against the traditional myopic approaches. Our results also confirmed a gradual increase in the joint radar-communications performance with increasing planning horizon length, which was expected in a non-myopic approach. Our numerical studies also confirmed that the ADP approach RS-MHP outperformed the NBO approach in terms of the target estimation rate.

REFERENCES CITED

[1] J. B. Evans, "Shared Spectrum Access for Radar and Communications (SSPARC)," *[Online]*. http://www.darpa.mil/program/shared-spectrum-access-for-radar-and-communications.

[2] D. W. Bliss and S. Govindasamy, *Adaptive Wireless Communications: MIMO Channels and Networks*. New York, New York: Cambridge University Press, 2013.

[3] D. W. Bliss, "Cooperative radar and communications signaling: The estimation and information theory odd couple," in *Proc. IEEE Radar Conference*, May 2014, pp. 50–55.

[4] B. Paul, A. R. Chiriyath, and D. W. Bliss, "Joint communications and radar performance bounds under continuous waveform optimization: The waveform awakens," in *IEEE Radar Conference*, May 2016, pp. 865–870.

[5] P. Chavali and A. Nehorai, "Cognitive radar for target tracking in multipath scenarios," in *Proc. Waveform Diversity & Design Conf.*, Niagara Falls, Canada, 2010.

[6] Ma, O., Chiriyath, A. R., Herschfelt, A., & Bliss, D. (2019). Cooperative Radar and Communications Coexistence Using Reinforcement Learning. In M. B. Matthews (Ed.), Conference Record of the 52nd Asilomar Conference on Signals, Systems and Computers, ACSSC 2018 (pp. 947-951).

This article has been accepted for publication in a future issue of this journal, but has not been fully edited. Content may change prior to final publication. Citation information: DOI 10.1109/TAES.2022.3162567, IEEE Transactions on Aerospace and Electronic Systems

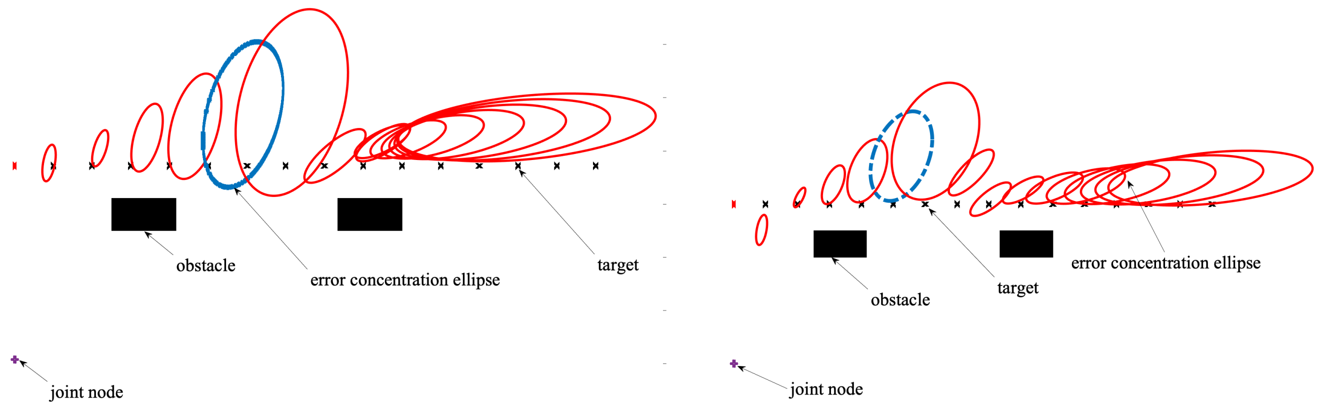

(a) Planning Horizon H=1

(b) Planning Horizon H=9

Fig. 7: Error concentration ellipse (95% confidence) of the dynamic target at different location in both myopic ($H = 1$) and non-myopic ($H > 1$) approaches for α = 0.5 by red lines. The number of iteration indexes is considered $k = 15$ to demonstrate which locations match which ellipses more precisely. For example, the solid blue line shows the error concentration ellipse at the time index $k = 5$ for $H = 1$, and the error concentration ellipse for $H = 9$ at the time index $k = 5$ is shown by the blue dotted line. We see that with the non-myopic method ($H > 1$), we could minimize the size of the error concentration ellipse as the target tracking error as determined by the spectral mask we chose.

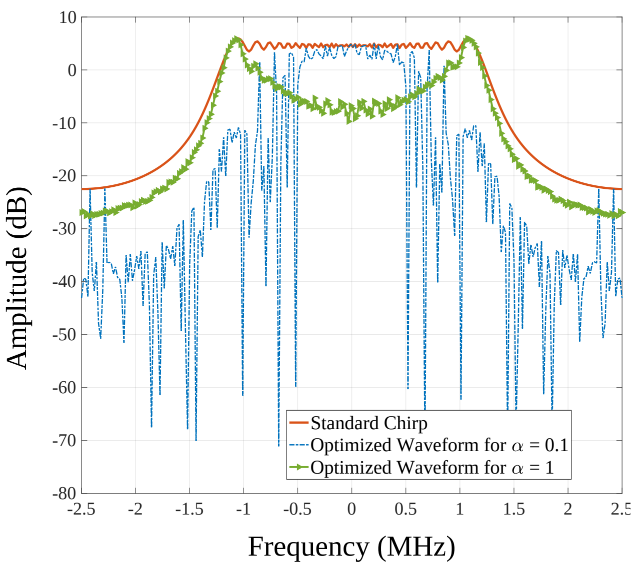

Fig. 8: The original unmasked chirp is depicted by the solid red line. The optimized waveform is depicted for $\alpha = 0.1$ by the blue dotted line. This waveform spectrum is communication-optimal and has more energy in the center of the bandwidth. The optimized waveform is depicted by the green dashed line for $\alpha = 1$ and, this waveform spectrum is radar-optimal and has more energy in the edges of the bandwidth.

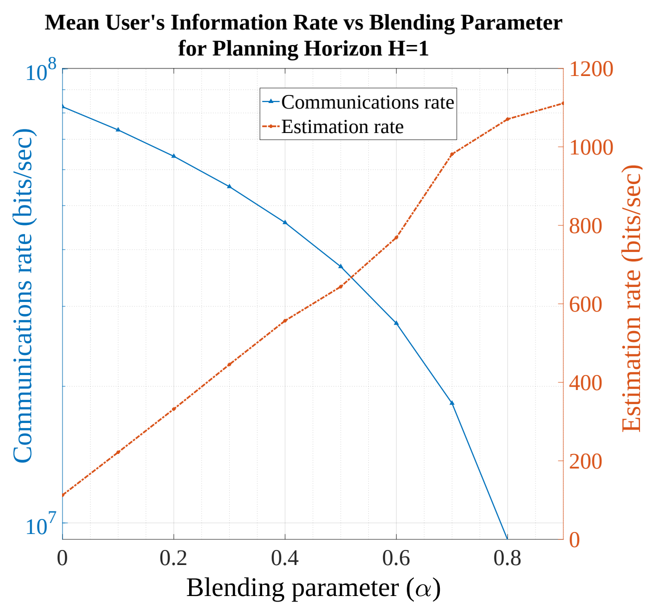

Fig. 9: Rate–rate curve depicting communications and estimation rate vs. α. Communications and estimation rate pairs are shown $\alpha \in [0, 1]$.

[7] E. K. P. Chong, C. Kreucher, and A. O. Hero, "Partially observable Markov decision process approximations for adaptive sensing,"*Disc. Event Dyn. Sys.*, vol. 19, pp. 377–422, 2009.

[8] S. A. Doly, A. Chiriyath, H. D. Mittelmann, D. W. Bliss, and S. Ragi, "A decision theoretic approach for waveform design in joint radar communications applications," in Proceedings of the 54th Asilomar Conference on Signals, Systems and Computers (Asilomar 2020), Pacific Grove, CA, Nov 01–04, 2020.

[9] S. Ragi and E. K. P. Chong, "UAV path planning in a dynamic environment via partially observable Markov decision process," *IEEE Trans. Aerosp. Electron. Syst.*,vol. 49, pp. 2397–2412, 2013.

[10] C. H. Papadimitriou and J. N. Tsitsiklis, The complexity of Markov decision processes,"Mathematics of Operations Research, vol. 12(3), pp. 441450, 1987."

[11] S. Ragi and H. D. Mittelmann, "Random-Sampling Multipath Hypothesis Propagation for Cost Approximation in Long-Horizon Optimal Control," in Proceedings of the 2020 IEEE Conference on Control Technology and Applications (CCTA), Montreal, Canada, August 24–26, 2020, pp. 14–18.

[12] S. Ragi and H. D. Mittelmann, "Random-Sampling Monte-Carlo Tree

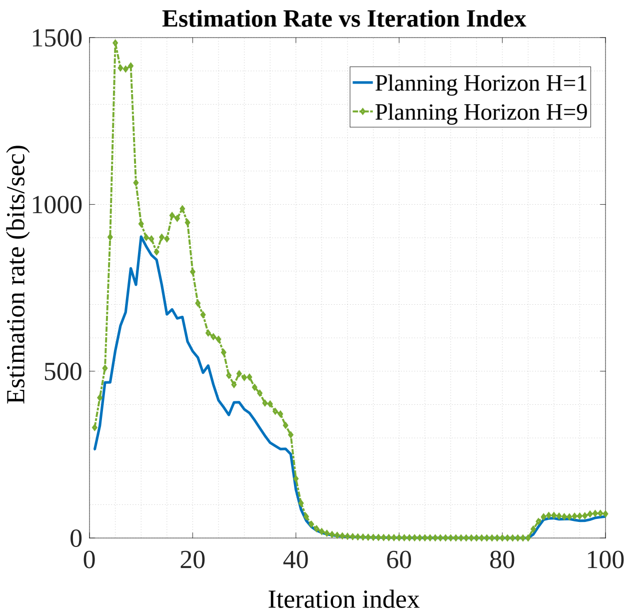

Fig. 10: Estimation rate vs. iteration index for both myopic and non-myopic approaches.

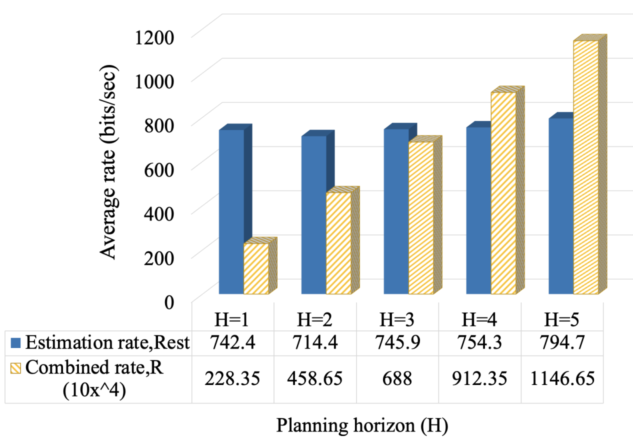

Fig. 11: Average estimation and communication rates vs. planning horizon $H \in \{1, 2, 3, 4, 5\}$.

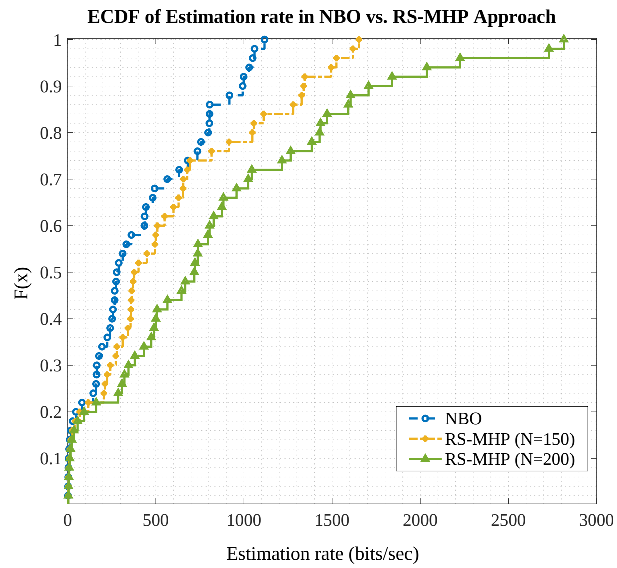

Fig. 12: Cumulative distribution of estimation rate for NBO vs. RS-MHP approaches. Here N represents the number of samples.

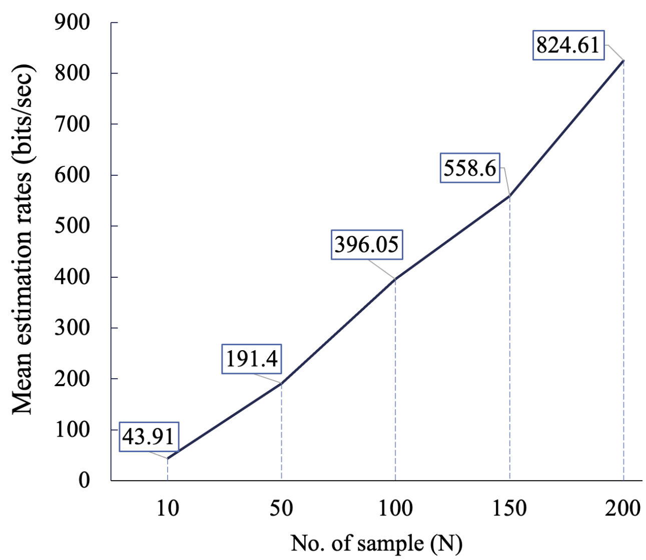

Fig. 13: Mean estimation rate vs. number of samples $N \in \{10, 50, 100, 150, 200\}$.

Search Methods for Cost Approximation in Long-Horizon Optimal Control," in IEEE Control Systems Letters, vol. 5, no. 5, pp. 1759-1764, Nov. 2021, doi: 10.1109/LCSYS.2020.3043991.

[13] S. Ragi, E. K. P. Chong, and H. D. Mittelmann, "Mixed-integer nonlinear programming formulation of a UAV path optimization problem," in *Proc. 2017 American Control Conf.*, Seattle, WA, 2017, pp. 406–411.

[14] A. Charlish and F. Hoffmann, "Anticipation in cognitive radar using stochastic control," in *Proc. IEEE Radar Conf.*, Arlington, VA, 2016, pp. 1692–1697.

[15] B. Paul, A. R. Chiriyath, and D. W. Bliss. Survey of rf communications and sensing convergence research. *IEEE Access*, 5:252–270, 2017.

[16] J. R. Guerci, R. M. Guerci, A. Lackpour, and D. Moskowitz, "Joint design and operation of shared spectrum access for radar and communications," in*IEEE Radar Conference*, May 2015, pp. 761–766.

[17] X. Wang, A. Hassanien, and M. G. Amin. Dual-function mimo radar communications system design via sparse array optimization. *IEEE Transactions on Aerospace and Electronic Systems*,55(3):1213–1226, June 2019.

[18] S. Zhou, X. Liang, Y. Yu, and H. Liu. Joint radar-communications co-use waveform design using optimized phase perturbation.*IEEE Transactions on Aerospace and Electronic Systems*,55(3):1227–1240, June 2019.

[19] F. Wang, H. Li, and M. A. Govoni. Power allocation and co-design of multicarrier communication and radar systems for spectral coexistence. *IEEE Transactions on Signal Processing*, 67(14):3818–3831,2019.

[20] A. Turlapaty and Y. Jin, "A joint design of transmit waveforms for radar and communications systems in coexistence," in *IEEE Radar Conference*, May 2014, pp. 315–319.

[21] M. Zatman and M. Scharrenbroich, "Joint radar-communications resource management," in *2016 IEEE Radar Conference (RadarConf)*, May 2016, pp.1–6.

[22] Y. L. Sit, C. Sturm, and T. Zwick, "One-stage selective interference cancellation for the OFDM joint radar-communication system," in *The 7th German Microwave Conference*, March 2012, pp. 1–4.

[23] G. C. Tavik, C. L. Hilterbrick, J. B. Evins, J. J. Alter, J. Joseph G. Crnkovich, J. W. de Graaf, W. H. II, G. P. Hrin, S. A. Lessin, D. C.

Wu, and S. M. Hagewood, "The advanced multifunction RF concept," *IEEE Transactions on Microwave Theory and Techniques*, vol. 53, no. 3, pp. 1009–1020, March 2005.

[24] L. Wang, J. McGeehan, C. Williams, and A. Doufexi, "Application of cooperative sensing in radar-communications coexistence," *IET Communications*,vol. 2, no. 6, pp. 856–868, July 2008.

[25] M. R. Bell, N. Devroye, D. Erricolo, T. Koduri, S. Rao, and D. Tuninetti, "Results on spectrum sharing between a radar and a communications system," in *2014 International Conference on Electromagnetics in Advanced Applications (ICEAA)*, August 2014, pp. 826–829.

[26] Marian Bica, Kuan-Wen Huang, Urbashi Mitra, and Visa Koivunen. Opportunistic radar waveform design in joint radar and cellular communication systems. In *IEEE Global Communications Conference (GLOBECOM)*, pages 1–7, December 2015.

[27] Alex Lackpour, Joseph R. Guerci, Alan Rosenwinkel, David Ryan, and Apurva N.Mody. Design and analysis of an information exchange-based radar/communications spectrum sharing system (RCS3). In *2016 IEEE Radar Conference (RadarConf)*, pages 1–6, May2016.

[28] C. D. Richmond, P. Basu, R. Learned, J. Vian, A. P. Worthen, and M. Lockard, "Performance bounds on cooperative radar and communication systems operation," in *2016 IEEE Radar Conference (RadarConf)*, May 2016, pp.1–6.

[29] M. P. Fitz, T. R. Halford, I. Hossain, and S. W. Enserink, "Towards simultaneous radar and spectral sensing," in *IEEE International Symposium on Dynamic Spectrum Access Networks (DYSPAN)*, April 2014, pp. 15–19.

[30] A. D. Harper, J. T. Reed, J. L. Odom, and A. D. Lanterman, "Performance of a joint radar-communication system in doubly-selective channels," in *49th Asilomar Conference on Signals, Systems and Computers*, November 2015, pp. 1369–1373.

[31] Simon Haykin. Cognitive radar: A way of the future. *IEEE Signal Processing Magazine*, 23(1):30–40, January 2006.

[32] J.R. Guerci. *Cognitive Radar: The Knowledge-aided Fully Adaptive Approach*. Artech House radar library. Artech House, 2010.

[33] Pawan Setlur, Natasha Devroye, "Adaptive waveform scheduling in radar: an information theoretic approach," Proc. SPIE 8361, Radar Sensor Technology XVI, 836103 (3 May 2012); https://doi.org/10.1117/12.919213

[34] Yogesh Nijsure, Yifan Chen, Chau Yuen, and Yong Huat Chew. Location-aware spectrum and power allocation in joint cognitive communication-radar networks. In *Sixth International ICST Conference on Cognitive Radio Oriented Wireless Networks and Communications (CROWNCOM)*, pages 171–175, June 2011.

[35] B. H. Kirk, R. M. Narayanan, K. A. Gallagher, A. F. Martone, and K. D. Sherbondy. Avoidance of time-varying radio frequency interference with software-defined cognitive radar. *IEEE Transactions on Aerospace and Electronic Systems*, 55(3):1090–1107, June 2019.

[36] Riccardo Palamà, Hugh Griffiths, and Francis Watson. Joint dynamic spectrum access and target-matched illumination for cognitive radar. *IET Radar, Sonar & Navigation*, 13:750–759(9), May 2019.

[37] Brandon Ravenscroft, Jonathan W. Owen, John Jakabosky, Shannon D. Blunt, Anthony F. Martone, and Kelly D. Sherbondy. Experimental demonstration and analysis of cognitive spectrum sensing and notching for radar. *IET Radar, Sonar & Navigation*, 12:1466–1475(9), December 2018.

[38] J. W. Owen, C. A. Mohr, B. H. Kirk, S. D. Blunt, A. F. Martone, and K. D. Sherbondy. Demonstration of real-time cognitive radar using spectrally-notched random fm waveforms. In *2020 IEEE International Radar Conference (RADAR)*, pages 123–128, 2020.

[39] B. Ravenscroft, J. W. Owen, B. H. Kirk, S. D. Blunt, A. F. Martone, K. D. Sherbondy, and R. M. Narayanan. Experimental assessment of joint range-doppler processing to addressclutter modulation from dynamic radar spectrum sharing. In *2020 IEEE International Radar Conference (RADAR)*, pages 448–453, 2020.

[40] A. Aubry, A. De Maio, M. Piezzo, M. M. Naghsh, M. Soltanalian, and P. Stoica. Cognitive radar waveform design for spectral coexistence in signal-dependent interference. In *IEEE Radar Conference*, pages 474–478, May 2014.

[41] Yogesh Nijsure, Yifan Chen, Said Boussakta, Chau Yuen, Yong Huat Chew, and Zhiguo Ding. Novel system architecture and waveform design for cognitive radar radio networks. *IEEE Transactions on Vehicular Technology*, 61(8):3630–3642, October 2012.

[42] Kuan-Wen Huang, Marian Bică, Urbashi Mitra, and Visa Koivunen. Radar waveform design in spectrum sharing environment: Coexistence and cognition. In *2015 IEEE Radar Conference*, pages 1698–1703, May 2015.

[43] A. F. Martone, K. A. Gallagher, and K. D. Sherbondy. Joint radar and communication system optimization for spectrum sharing. In *2019 IEEE Radar Conference*, pages 1–6, 2019.

[44] S. Howard, W. Moran, A. Calderbank, H. Schmitt, and C. Savage, "Channel parameters estimation for cognitive radar systems," in *Proceedings IEEE International Conference on Acoustics, Speech, and Signal Processing*, vol. 5, March 2005, pp. 897–900.

[45] S. Howard, A. Calderbank, and W. Moran, "The finite Heisenberg-Weyl groups in radar and communications," vol. 2006, pp. 1–12, April 2006.

[46] A. Pezeshki, A. R. Calderbank, W. Moran, and S. D. Howard, "Doppler resilient Golay complementary waveforms," *IEEE Transactions on Information Theory*, vol. 54, no. 9, pp. 4254–4266, September 2008.

[47] L. Xiaobai, Y. Ruijuan, Z. Zunquan, and C. Wei, "Research of constructing method of complete complementary sequence in integrated radar and communication," in *IEEE 11th International Conference on Signal Processing (ICSP)*, vol. 3, October 2012, pp. 1729–1732.

[48] M. Braun, C. Sturm, A. Niethammer, and F. K. Jondral, "Parametrization of joint OFDM-based radar and communication systems for vehicular applications," in *IEEE 20th International Symposium on Personal, Indoor and Mobile Radio Communications*, September 2009, pp. 3020–3024.

[49] C. Sturm, T. Zwick, and W. Wiesbeck, "An OFDM system concept for joint radar and communications operations," in *IEEE 69th Vehicular Technology Conference*, April 2009, pp. 1–5.

[50] Y. L. Sit, C. Sturm, L. Reichardt, T. Zwick, and W. Wiesbeck, "The OFDM joint radar-communication system: An overview," in *The Third International Conference on Advances in Satellite and Space Communications*, April 2011, pp. 69–74.

[51] Y. L. Sit, L. Reichardt, C. Sturm, and T. Zwick, "Extension of the OFDM joint radar-communication system for a multipath, multiuser scenario," in *2011 IEEE RadarCon (RADAR)*, May 2011, pp. 718–723.

[52] C. W. Rossler, E. Ertin, and R. L. Moses, "A software defined radar system for joint communication and sensing," in *IEEE Radar Conference (RADAR)*,May 2011, pp. 1050–1055.

[53] T. Guo and R. Qiu, "OFDM waveform design compromising spectral nulling,side-lobe suppression and range resolution," in *IEEE Radar Conference*, May 2014, pp. 1424–1429.

[54] S. C. Thompson and J. P. Stralka, "Constant envelope OFDM for power-efficient radar and data communications," in *International Waveform Diversity and Design Conference*, February 2009, pp. 291–295.

[55] R. F. Tigrek, W. J. A. de Heij, and P. van Genderen, "Relation between the peak to average power ratio and Doppler sidelobes of the multi-carrier radar signal," in *International Radar Conference - Surveillance for a Safer World*, October 2009, pp. 1–6.

[56] Thornton, C. E.; Buehrer, R. M.; Martone, A. F. & Sherbondy, K. D., "Experimental Analysis of Reinforcement Learning Techniques for Spectrum Sharing Radar," 2020 IEEE International Radar Conference (RADAR), 2020, 67-72

[57] T. M. Cover and J. A. Thomas, *Elements of Information Theory*,2nd ed. Hoboken, New Jersey: John Wiley & Sons, 2006.

[58] A. R. Chiriyath, B. Paul, G. M. Jacyna, and D. W. Bliss, "Inner bounds on performance of radar and communications co-existence,"*IEEE Transactions on Signal Processing*, vol. 64, no. 2, pp. 464–474, January 2016.

[59] B. Paul and D. W. Bliss, "Extending joint radar-communications bounds for FMCW radar withDoppler estimation," in *IEEE Radar Conference*, May 2015, pp.89–94.

[60] B. Paul and D. W. Bliss, "The constant information radar," *Entropy*,vol. 18, no. 9, p. 338, 2016. [Online]. Available: http://www.mdpi.com/1099-4300/18/9/338

[61] MATLAB's fmincon. 2016. [Online]. Available: https://www.mathworks.com/help/optim/ug/fmincon.

This article has been accepted for publication in a future issue of this journal, but has not been fully edited. Content may change prior to final publication. Citation information: DOI 10.1109/TAES.2022.3162567, IEEE Transactions on Aerospace and Electronic Systems

Shammi A. Doly received her B.Sc.(Eng) degree in Electrical and Electronic Engineering from Ahsanullah University of Science and Technology, Dhaka, Bangladesh, in 2015. She received the MS. degree in Electrical Engineering from South Dakota School of Mines, Rapid City, SD, USA, in 2021.

Currently, she is a Ph.D. student with BLISS Lab and WISCA at Arizona State University, Tempe, USA. Before joining BLISS Lab, Shammi worked at Unmanned & Swarm System LAB as a research assistant in South Dakota School of Mines with Dr. Shankarachary Ragi. Her current research interests include distributed-coherent systems and optimal control.

Alex Rajan Chiriyath received his B.S.E.E. degree (Cum Laude) in electrical engineering from the University of Michigan at Ann Arbor, Ann Arbor, MI, USA, in 2012 and the M.S. degree and Ph.D. degree in electrical engineering from Arizona State University, Tempe, AZ, USA, in 2014 and 2018.

He joined Arizona State University as a Postdoctoral Researcher in 2018. He is currently an Assistant Research Professor with BLISS Labs and WISCA at Arizona State University since 2021. His main research interest includes RF spectral convergence and flexible, multi-function RF systems.

Hans Mittelmann is a professor of Computational Mathematics at Arizona State University. Prior to his appointment he was a professor at the University of Dortmund/Germany. He has a PhD in Mathematics from the Technical University of Darmstadt/Germany, where he also obtained the Habilitation.

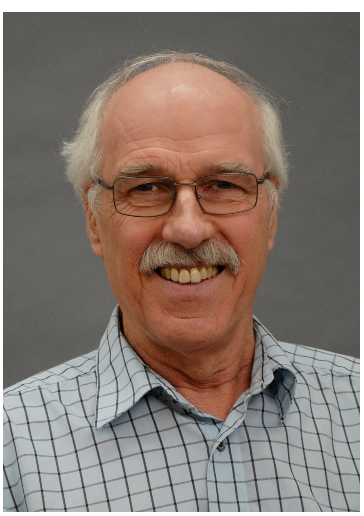

He has written 160 papers in Computational Mathematics, initially in the numerical solution of partial differential equations, lately in interdisciplinary collaboration concentrating on optimization and applications. For more than twenty years he is maintaining two of the most frequented websites on optimization and related software. He evaluates a wide range of available programs for continuous and discrete optimization.

This article has been accepted for publication in a future issue of this journal, but has not been fully edited. Content may change prior to final publication. Citation information: DOI 10.1109/TAES.2022.3162567, IEEE Transactions on Aerospace and Electronic Systems

Prof. Daniel W. Bliss (bliss.asu.edu) is the Motorola Professor at Arizona State University in the school of Electrical, Computer, and Energy Engineering and is the Director of ASU's Center for Wireless Information Systems and Computational Architectures (WISCA). He received his Ph.D. in Physics from the University of California at San Diego (1997), and his B.S. in Electrical Engineering from ASU (1989). He is a Fellow of the IEEE and received the 2021 IEEE Warren D. White Award for Excellence in Radar Engineering. He is a member of the IEEE Signal Processing Magazine Editorial Board. He has published two textbooks and more than 200 technical articles.

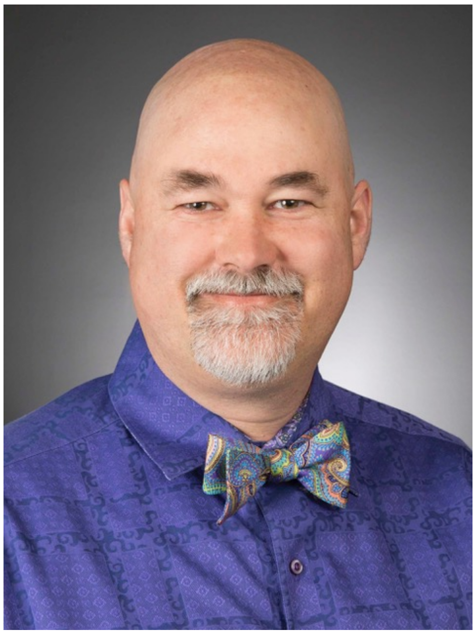

He is responsible for foundational work in electronic protection, adaptive MIMO radar, MIMO communications, distributed-coherent systems, and RF convergence. To enable implementation of these advanced systems, he has led coarse-scale heterogeneous system-on-chip (SoC) development programs.

He has served as Principal Investigator on numerous projects including sponsored programs with DARPA, ONR, Google, Airbus, and many others. Before joining ASU, he was a Senior Member of the Technical Staff at MIT Lincoln Laboratory (1997-2012).

Between his undergraduate and graduate degrees, Dan was employed by General Dynamics (1989-1993), where he designed avionics for the Atlas-Centaur launch vehicle and performed magnetic field optimization for high-energy particle-accelerator superconducting magnets. His doctoral work (1993-1997) was in the area of high-energy particle physics and lattice-gauge-theory calculations.

Shankarachary Ragi is an assistant professor in the Electrical Engineering Department at South Dakota Mines, USA. He earned his Ph.D. degree in Electrical and Computer Engineering at Colorado State University, USA in 2014, and his B.Tech. and M.Tech. degrees in Electrical Engineering at Indian Institute of Technology Madras, India in 2009. Before joining South Dakota Mines, Ragi has worked as a postdoctoral researcher in the mathematics department at Arizona State University, and prior to that, he worked as a Senior Controls Engineer at Cummins Emission Solutions.

His current research interests include machine learning, image analysis, robotics, and optimal control. Ragi has served as an Associate Editor for IEEE Access during 2017-2020. He has authored or co-authored over 29 peer-reviewed publications in various journals and conference proceedings. He is a senior member of the IEEE.